Multiple-Complex Coefficient-Filter-Based PLL for Improving the Performance of Shunt Active Power Filter under Adverse Grid Conditions

Terriche, Yacine; Golestan, Saeed; Guerrero, Josep M.; Quintero, Juan Carlos Vasquez

Published in:
Proceedings of the 2018 IEEE Power & Energy Society General Meeting (PESGM)

DOI (link to publication from Publisher):
10.1109/PESGM.2018.8586172

Publication date:
2018

Document Version
Accepted author manuscript, peer reviewed version

Multiple-Complex Coefficient-Filter-Based PLL for Improving the Performance of Shunt Active Power Filter under Adverse Grid Conditions

Yacine Terriche, Saeed Golestan, Josep M. Guerrero, Juan C. Vasquez

Department of Energy Technology, Aalborg University, Aalborg, Denmark
(yte@et.aau.dk; sgd@et.aau.dk; joz@et.aau.dk; juq@et.aau.dk

***Abstract*—In recent years, shunt active power filters (SAPFs) are becoming a popular solution for power quality issues. A crucial part in synchronizing the SAPFs is the accurate estimation of the grid phase/frequency. The synchronous reference frame phase-locked loop (SRF-PLL) is a commonly used technique for this issue due to its simplicity and robustness under ideal grid conditions. However, the tradeoff between the accuracy and the fast transient response of the SRF-PLL becomes a serious problem under distorted and unbalanced grid conditions. To overcome this challenge, several advanced PLLs have been proposed in the literature. The multiple-complex coefficient-filter-based PLL (MCCF-PLL) has interesting features under adverse grid condition. The unique distinction of the MCCF-PLL from other PLLs is the ability of providing information about the sequence (polarity) of each individual frequency. However, the MCCF-PLL has not received much attention in APFs. In this paper, a study and an implementation of a selective harmonic cancelation technique based on MCCF-PLL to the SAPF is suggested. The proposed method proved its reliability and robust behavior in optimizing the performance of the SAPF under unbalanced and distorted grid conditions. Simulation results are carried out under MATLAB\Simulink, then validated experimentally and compared with SRF-PLL.**

***Index Terms*— Frequency and phase detection, multiple complex-coefficient filter (MCCF), phase-locked loop (PLL), power quality issues, shunt active power filter (SAPF), synchronization.**

I. INTRODUCTION

THE power quality issues have become a vital subject due to the proliferation of non-linear loads applied for the power electronic control. The harmonic components drawn by these loads highly increase the losses and disturb the voltage quality [1]. To deal with these power quality issues, the APFs are becoming an attractive solution due to their flexibility, fast dynamic response during load variation, the ability of decreasing the total harmonic distortion (THD) significantly using only one inverter, and the capability of compensating for the unbalance and the power factor (PF) [2]-[3]. The APFs have different topologies. The shunt APF which is focused on this paper is connected in parallel with the source, and generates the harmonic and the reactive contents demanded by the loads, and consequently the source will generate only the active power [4], [5]. Identifying the reference compensating current (RCC) is a crucial matter in controlling the APF. The synchronous reference frame (SRF) approach is widely applied to the APFs for extracting the RCC [6]-[8]. This method, which is a time-domain method, is distinguished form the frequency-domain methods by its simplicity, fast dynamic response and low computation burden. Moreover, the PF and the current unbalance can be easily compensated using the SRF approach.

An essential issue in applying the SRF approach and synchronizing the RCC is the estimation of the grid voltage phase. Several synchronization methods have been proposed in the literature for this purpose. These methods can be classified as closed-loop and open-loop methods [9]. The open-loop synchronization methods are unconditionally stable, and provide an acceptable performance with regard to frequency/phase estimation and preciseness if the grid frequency is close to its nominal value. However, their performance degrades under large frequency deviations. The closed-loop synchronization methods are distinguished by a closed-loop phase or frequency feedback control system. This feedback regulates the error between the estimated phase/frequency and the reference towards zero. Probably, the most popular closed-loop synchronizing method for APFs is using a PLL. The SRF-PLL is a standard PLL for grid-connected applications. Under ideal grid conditions, the SRF-PLL provides accurate information of the phase and the amplitude of the grid voltage with a fast transient response. On the other hand, the SRF-PLL can also estimate the grid frequency to adapt the filters of extracting the harmonic components to the grid frequency changes. However, under adverse grid voltage conditions, the performance of the SRF-PLL is tended to worsen. Reducing the loop bandwidth of the SRF-PLL makes it possible to work under harmonically contaminated voltage. Nevertheless, this solution is attained at the cost of the speed of the transient response that is unwanted in several applications. Moreover, the performance of this solution decreases in the presence of voltage unbalance. Several Advanced PLLs have been proposed in the literature to overcome the weaknesses of the SRF-PLL under adverse grid conditions. In [10], a dual second-order generalized integrator PLL (DSOGI-PLL) is presented, the principle lies in using Clarke transform to operate the filtering process, this latter is performed using DSOGI-based quadrature signal generator in the presence of harmonic components and unbalance, then the estimated fundamental positive sequence is served to the SRF-PLL, after that, the estimated frequency is fed back to be adaptive.

In [11] an adaptive resonant filter is integrated in the SRF-PLL with a simple structure. This idea can optimize the accuracy and the dynamic response of the SRF-PLL under adverse grid condition and frequency drift. An adaptive SRF-PLL that is supported by several notch filters (NFs) is presented in [12]. Based on Schur-lattice structure, this PLL can significantly reject the ripples caused by the harmonic components and the unbalance under nominal and off-nominal frequency. The incorporation of the moving average filter into the SRF-PLL (MAF-PLL) is relatively advanced [13], when performing Park transform, the fundamental positive sequence component appears as a dc component, the application of the MAF-PLL yields to separate between the fundamental components and the ripples, if the window width of the MAF is appropriately selected, all the harmonics and the fundamental negative sequence are blocked. In this case, the MAF can be considered as a quasi-ideal low-pass filter [14]. In [15], the application of cascaded delayed signal cancelation based PLL (CDSC-PLL) enables the cancelation of the desired harmonic components, the CDSC structure can be arranged in parallel to provide a selective harmonic rejection with less sensitivity to slight frequency variation. Other techniques are summarized in [16]. The complex-coefficient filters (CCFs) have interesting features of making the distinction between the positive and negative sequences of the same frequency [17]. Guo *et al.* has presented a novel structure of the PLL based on CCFs named multiple CCF PLL (MCCF-PLL) [18]. This structure is based on implementing a range of submodules that work in a cooperative manner to provide the sequence selectivity of the desired harmonic components. Moreover, the application of the CCFs to the PLL provides accurate frequency/phase estimation with a fast transient response under adverse grid conditions.

This paper suggests a selective harmonic cancelation technique based on the MCCF-PLL to improve the dynamic performance of the SAPF under distorted and unbalanced grid conditions [18]. The advantage of applying the MCCF-PLL lies in providing information about each harmonic component with its corresponding sequence. Based on the SRF approach, the load currents are transformed from the *abc* stationary system into the *dq* rotating frame. Then, the separation between the dc components and the ripples is achieved using the MAF. After that, the RCC are obtained by transforming back the extracted ripples from the *dq* rotating frame to *abc* stationary system. The Park transform is achieved by estimating the phase of the distorted and unbalanced grid voltage using the MCCF-PLL. The role of this latter is to extract the fundamental positive sequence of the affected grid voltage, and feed it to the SRF-PLL to estimate its phase and frequency. The number of CCFs is set according to the number of the dominant existing harmonic components. The estimated frequency is fed back to adapt the CCFs during frequency deviation. The effectiveness of the proposed technique is verified by simulation under MATLAB\Simulink environment and validated experimentally and compared with a standard SRF-PLL.

II. MCCF-PLL

The MCCF-PLL is an advanced SRF-PLL that is distinguished by a pre-filtering stage in the stationary $\alpha\beta$ frame. This pre-

filtering stage contains several submodules of the CCFs operating in a cooperative manner as shown in Fig. 1 [18]. If the grid voltage is unbalanced but slightly affected by harmonics, two-module (TM) system tuned at the positive and negative sequences of the fundamental frequency can be efficient. However, under high harmonic contamination, the implementation of multiple-module (MM) system that is shown in Fig.1 is recommended [18], [19].

An unbalanced and harmonically contaminated three-phase voltage can be represented as

$$V_{s1}(t) = \sum_{h=1}^{m} v_h^p \cos\left(hwt + \phi_h^p\right) + v_h^n \cos(hwt + \phi_h^n) \quad (1)$$

$$V_{s2}(t) = \sum_{h=1}^{m} v_h^p \cos\left(hwt + \phi_h^p - \frac{2\pi}{3}\right) + v_h^n \cos\left(hwt + \phi_h^n + \frac{2\pi}{3}\right) \quad (2)$$

$$V_{s3}(t) = \sum_{h=1}^{m} v_h^p \cos\left(hwt + \phi_h^p + \frac{2\pi}{3}\right) + v_h^n \cos\left(hwt + \phi_h^n - \frac{2\pi}{3}\right) \quad (3)$$

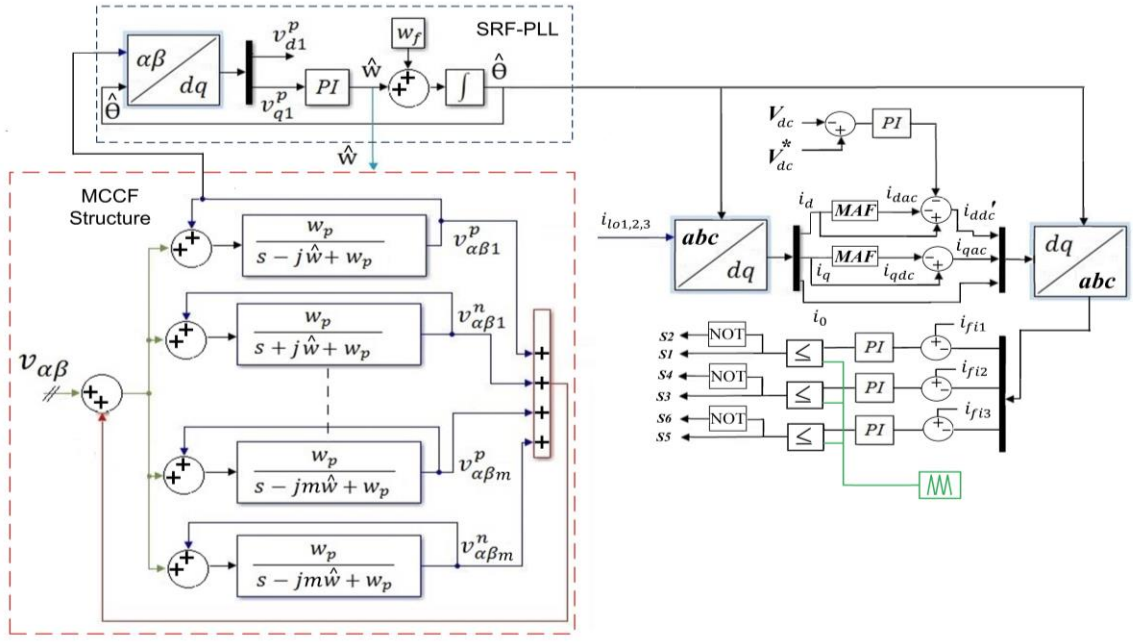

(a)

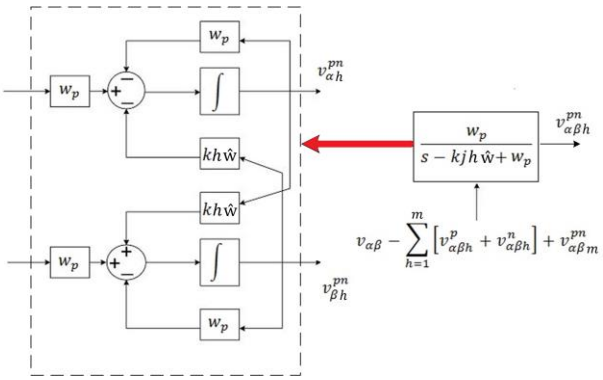

(b)

Fig. 1. control structure of the SAPF synchronized using MCCF-PLL. (a) Schematic diagram of the control structure. (b) A single submodule of the MCCF

where $v_h^p,\ v_h^n,\ \phi_h^p,\ \phi_h^n$ are respectively the amplitudes and the phase angles of the positive and negative sequences that correspond to the hth harmonic component of the contaminated grid voltage. Transforming these voltages from *abc* to $\alpha\beta$ using Clarke transform results in

$$\begin{bmatrix} v_\alpha(t) \\ v_\beta(t) \end{bmatrix} = \begin{bmatrix} v_\alpha^p(t) + v_\alpha^n(t) \\ v_\beta^p(t) + v_\beta^n(t) \end{bmatrix} = [\mathrm{T}] \begin{bmatrix} V_{s1}(t) \\ V_{s2}(t) \\ V_{s3}(t) \end{bmatrix} \tag{4}$$

Where

$$[\mathrm{T}] = \frac{2}{3}\begin{bmatrix} 1 & \frac{-1}{2} & \frac{-1}{2} \\ 0 & \frac{\sqrt{3}}{2} & \frac{-\sqrt{3}}{2} \end{bmatrix}$$

$$\left[v_\alpha^p(t) + v_\alpha^n(t)\right] = \sum_{h=1}^m v_{\alpha h}^p(t) + \sum_{h=1}^m v_{\alpha h}^n(t) \ = \sum_{h=1}^m v_h^p \cos\left(hwt + \phi_h^p\right) + \sum_{h=1}^m v_h^n \cos(hwt + \phi_h^n) \tag{5}$$

$$\left[v_\beta^p(t) + v_\beta^n(t)\right] = \sum_{h=1}^m v_{\beta h}^p(t) + \sum_{h=1}^m v_{\beta h}^n(t) = \sum_{h=1}^m v_h^p \sin\left(hwt + \phi_h^p\right) - \sum_{h=1}^m v_h^n \sin(hwt + \phi_h^n) \tag{6}$$

Applying the transformation of Park ($\alpha\beta$-to-dq) yields

$$\begin{bmatrix} v_d(t) \\ v_q(t) \end{bmatrix} = \begin{bmatrix} v_d^p(t) + v_d^n(t) \\ v_q^p(t) + v_q^n(t) \end{bmatrix} = [\mathrm{T_1}] \begin{bmatrix} v_\alpha(t) \\ v_\beta(t) \end{bmatrix} \tag{7}$$

Where

$$[\mathrm{T_1}] = \begin{bmatrix} \cos\left(\hat{\theta}\right) & \sin\left(\hat{\theta}\right) \\ -\sin\left(\hat{\theta}\right) & \cos\left(\hat{\theta}\right) \end{bmatrix},\ \hat{\theta} = \hat{w}t + \hat{\phi}_1^p$$

$$\left[v_d^p(t) + v_d^n(t)\right] = \sum_{h=1}^m v_{dh}^p(t) + \sum_{h=1}^m v_{dh}^n(t) = \sum_{h=1}^m v_h^p \cos\left((hw - \hat{w})t + \phi_h^p - \hat{\phi}_1^p\right) + \sum_{h=1}^m v_h^n \cos\left((hw + \hat{w})t + \phi_h^n + \hat{\phi}_1^p\right) \tag{8}$$

$$\left[v_q^p(t) + v_q^n(t)\right] = \sum_{h=1}^m v_{qh}^p(t) + \sum_{h=1}^m v_{qh}^n(t) = \sum_{h=1}^m v_h^p \sin\left((hw - \hat{w})t + \phi_h^p - \hat{\phi}_1^p\right) - \sum_{h=1}^m v_h^n \sin\left((hw + \hat{w})t + \phi_h^n + \hat{\phi}_1^p\right) \tag{9}$$

Under a quasi-locked condition ($\hat{\phi}_1^p \approx \phi_1^p$ and $\hat{w} = w$) (7) becomes

$$\begin{bmatrix} v_d \\ v_q \end{bmatrix} = \begin{bmatrix} v_{ddc} \\ v_{qdc} \end{bmatrix} + \begin{bmatrix} v_{dac} \\ v_{qac} \end{bmatrix} \tag{10}$$

Where v_{ddc} and v_{qdc} are the dc terms, while v_{dac} and v_{qac} are the disturbance terms.

Fig. 1(a) shows the control structure of the SAPF that is based on the MCCF-PLL for performing the synchronization. The contaminated voltage $V_{s1,2,3}$ is transformed from *abc* stationary system to $\alpha\beta$ using (4)-(6). Then, the MCCF structure based on CCFs is applied to extract the fundamental positive sequences ($v^p_{\alpha\beta1}$) of the distorted voltages $v_{\alpha\beta}$. After that, $v^p_{\alpha\beta1}$ are fed to the SRF-PLL to estimate the phase angle of the fundamental positive sequence of $V_{s1,2,3}$. Next, the estimated phase angle is served to SRF approach to perform Park transformation of the load currents ($i_{l1,2,3}$), while the estimated frequency is fed back to adapt the CCFs tuning frequency. In the rotating *dq* frame, the fundamental currents (i_{ddc}) and (i_{qdc}) appear as a dc components while the harmonic components (i_{dac}) and (i_{qac}) appear as ripples. The separation between the fundamental components and the ripples is achieved using the MAF. The window width (T_w) of the MAF is selected according to the type of the current perturbation. In the case of existence of the harmonics $6h \pm 1$, selecting T_w to $\frac{1}{6}$ cycle offers fast time response with sufficient accuracy. When only odd harmonics exist, T_w has to be set to $\frac{1}{2}$ cycle for improving the accuracy. When, in addition to odd harmonics, dc offset and even harmonics appear, then setting T_w to one cycle is necessary. The dc link voltage V_{dc} is compared with a reference, and the error is added to i_{dac} through a PI controller to force V_{dc} to follow its reference. The RCC are obtained by transforming i'_{dac} and i_{qac} back from the *dq* rotating frame to the *abc* stationary frame. Finally, the RCC are compared with the output filter currents ($i_{fi1,2,3}$) of the SAPF and the error is fed to the PWM control through the PI controller. The triangular signal of the PWM control is set to 7 kHz. The advantage of the PI controller lies in its simplicity in mitigating the error, and the effectiveness in optimizing the dynamic response of the SAPF.

Fig. 1(b) depicts the basic structure of each CCF tuned at hth harmonic component. For extracting the positive sequence of $v_{\alpha\beta h}$, K is set to 1 and for extracting the negative sequence of $v_{\alpha\beta h}$, K is set to -1. According to Fig. 1(b), the fundamental positive sequences $v^p_{\alpha1}$ and $v^p_{\beta1}$ can be expressed as:

$$v^p_{\alpha1} = \frac{w_p}{s - j\widehat{\mathrm{w}} + w_p} \times \left(v_\alpha - \sum_{h=1}^{m} \left[v^p_{\alpha h} + v^n_{\alpha h} \right] + v^p_{\alpha1} \right) \tag{11}$$

$$v^p_{\alpha1} = \frac{w_p}{s + w_p} \times \left(v_\alpha - \sum_{h=2}^{m} v^p_{\alpha h} - \sum_{h=1}^{m} v^n_{\alpha h} \right) - \frac{\widehat{\mathrm{w}}}{s + w_p} \times v^p_{\beta1} \tag{12}$$

$$v^p_{\beta1} = \frac{w_p}{s - j\widehat{\mathrm{w}} + w_p} \times \left(v_\beta - \sum_{h=1}^{m} \left[v^p_{\beta h} + v^n_{\beta h} \right] + v^p_{\beta1} \right) \tag{13}$$

$$v^p_{\beta1} = \frac{w_p}{s + w_p} \times \left(v_\beta - \sum_{h=2}^{m} v^p_{\beta h} - \sum_{h=1}^{m} v^n_{\beta h} + v^p_{\beta1} \right) + \frac{\widehat{\mathrm{w}}}{s + w_p} \times v^p_{\alpha1} \tag{14}$$

According to [19], the MCCF-PLL based on two submodules tuned at the fundamental positive and negative sequence

components is equivalent to the multiple reference frame based PLL (MRF-PLL) [21], which implies that the linearized model of the MRF-PLL can be implemented for the MCCF-PLL. But in case of using several submodules, the disturbance input to the linearized model is changed according to the number of CCFs.

The difference between real band-pass filters (RBFs) and complex band-pass filters (CBFs) lies in the sequence selectivity. The real coefficient filters cannot distinguish between the polarity of the aimed frequency, and thus pass both sequences (for example +250 Hz and -250 Hz), while the CBFs have the unique feature of selecting the sequence of each frequency.

A typical complex bandpass filter (CBF) can be expressed in (15) for the positive sequence and in (16) for the negative sequence of the aimed frequency.

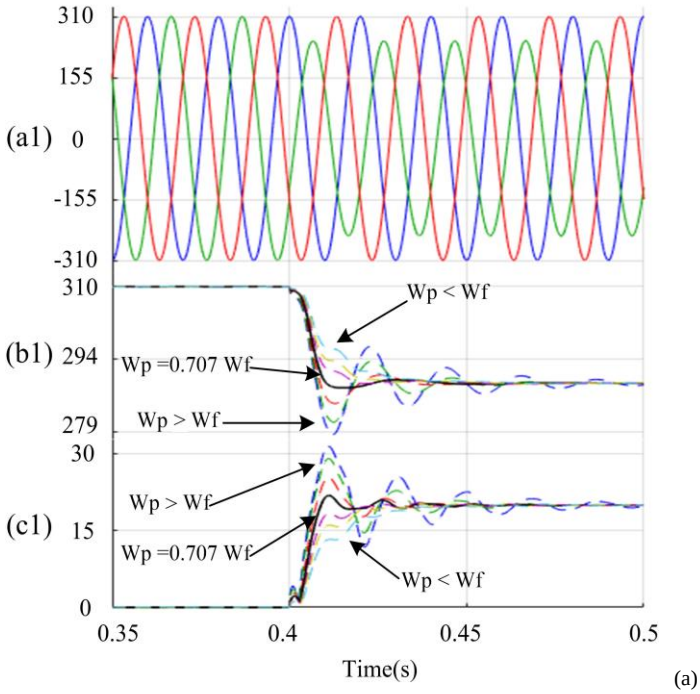

(a)

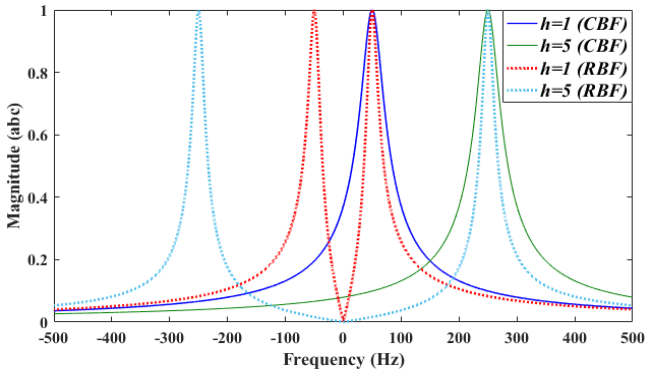

(b)

Fig. 2. Dynamic response and tuning behavior of the CBF. (a) analysis of w_p effect on the CBF dynamic behavior. (a1) grid voltage, (b1) the positive sequence of the fundamental frequency and (c1) is the negative sequence of the fundamental frequency. (b) Bode plot of a first-order CBF and a second-order RBF

$$G_F{}^p(s) = \frac{w_p}{s - jh\hat{w} + w_p} \tag{15}$$

$$G_F{}^n(s) = \frac{w_p}{s + jh\hat{w} + w_p} \tag{16}$$

where $\hat{w}$ is the estimated frequency.

For an optimum damping ration (well-damped with fast transient response), w_p is set equal to $0.707w_f$ [20]. In order to confirm the optimum choice of w_p, Fig. 2(a) is presented. Several values of w_p are assessed in extracting the positive and negative sequences of the fundamental frequency ($w_p = [2w_f, 1.5w_f, w_f, 0.707w_f, 0.5w_f, 0.3w_f, 0.2w_f]$) under an unbalanced grid voltage. When the grid voltage subjects to an asymmetrical voltage sag, it is obvious that the values of w_p that are higher than $0.707w_f$ result in a fast dynamic response with large oscillations, while the values of w_p that are less than $0.707w_f$ offer a slow and damped dynamic response. Therefore, the optimum choice of w_p is set to $0.707w_f$ since it provides a suitable compromise between the overshoot and settling time. Fig. 2(b) depicts the Bode magnitude diagram of a typical first-order CBF and a typical second-order RBF tuned at the fundamental and 5th harmonic frequencies. The damping ratio ξ is set to 0.707 and w_p is set to 222.11 rad/s. It is clear that the attenuation ratio of both polarities (positive and negative sequences) attained by the second-order BPF for both frequencies (fundamental and 5th harmonic) are 1, which implies that both sequences of each frequency (+50 Hz, +250 Hz, -50 Hz, -250Hz) pass the filters. However, the CCF bode magnitude diagram depicted using (15), offers a unit gain at only the positive sequences of the fundamental and the 5th harmonic frequency, with a certain filtering at the adjoining frequencies, and a zero phase shift.

According to [19], designing the PI parameters is attained by extracting the open loop transfer function of the small-signal model of the MCCF-PLL that is shown in Fig. 3.

$$G_{OLM}(s) = \frac{\hat{\phi}_1^p(s)}{\phi_e(s)}\Big|_{v_{qac(s)=0}} = v_1^p k_p w_p \frac{s + (k_i/k_p)}{s^2(s + w_p)} \tag{18}$$

The controller gains k_p and k_i are selected based on the extended symmetrical optimum method [22], [23]. Details of selecting the gains k_i and k_p are well explained in [19].

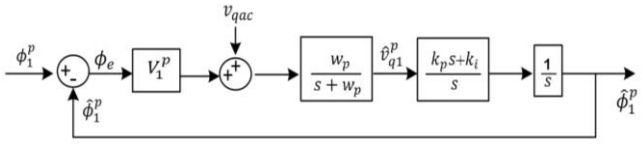

Fig. 3. Small signal model of the MCCF-PLL

III. Simulation Results

A. *Behavior of the MCCF-PLL Under Unbalanced and Distorted Gird Voltage and Frequency Excursion*

The study of the MCCF-PLL is attained under MATLAB/Simulink environment. The CCFs are not adapted with the frequency feedback to evaluate their performance under a small frequency excursion. Before the instance 0.1s, the grid voltage RMS value is set to 220V, the unbalance is caused by reducing the second phase value to 10% from its nominal value, and the -5th and +7th harmonic components are superposed on the voltage with the values of 12.4V. After the instance 0.1s, the unbalance is increased by reducing the second phase value to 30% from its nominal value, and the values of the -5th and +7th harmonic components are increased to 31.1V. In the instance 0.15s, the grid frequency is drifted from 50 Hz to 52 Hz. w_p is set equal to 0.707ŵ to provide an optimum damping ratio, the PI controller gains of the MCCF-PLL are set to kp =220 and ki =2400.

Fig. 4(a) presents the performance of the MCCF-PLL under unbalanced and distorted grid condition and grid frequency variation using TM structure. Before the instance 0.1s, the unbalance and distortion of $V_{s1,2,3}$ is relatively small. It is observed that the extracted fundamental positive sequence $v_{\alpha 1}^{p}$ is sinusoidal, while the fundamental negative sequence $v_{\alpha 1}^{n}$ is relatively contaminated. The estimated frequency of the MCCF-PLL using TM structure contains small ripples comparing to the estimated frequency of the SRF-PLL. In the instance 0.1s, the unbalance and the distortion of $V_{s1,2,3}$ increase and cause more affection to $v_{\alpha 1}^{n}$, while the distortion of $v_{\alpha 1}^{p}$ increases slightly and almost neglected. This can be clearly depicted on the small increase of the ripples in the estimated frequency, whereas the augmentation of the ripples in the estimated frequency using the SRF-PLL is relatively large. When the frequency deviation occurs in the instance 0.15s, it is clear that the waveform of $v_{\alpha 1}^{p}$ and the frequency are not affected, while the transient response of the phase error and the frequency takes approximately less than two cycles to reach steady state.

Fig. 4(b) demonstrates the performance of the MCCF-PLL under unbalanced and distorted grid condition and grid frequency variation using MM structure tuned for the fundamental frequency positive and negatives sequences and the most dominant harmonic components (-5th and +7th). Before the perturbation increases, $v_{\alpha 1}^{p}$ and $v_{\alpha 1}^{n}$ are accurately extracted with a sinusoidal waveform and the estimated frequency is filtered from ripples. When the voltage perturbation occurs in the instance 0.1s, $v_{\alpha 1}^{p}$ is not affected by the perturbation, while $v_{\alpha 1}^{n}$is slightly affected and takes almost the sinusoidal waveform. On the other hand, the estimated frequency is continues before the perturbation occurs, then slight ripples that can be considered neglected appear on it during the perturbation, while the estimated frequency of the SRF-PLL contains large ripples that increase significantly when the perturbation occurs. The last subplots of Fig. 4(b) depict respectively the information of the superposed harmonic components (-5th and 7th) extracted by the MCCF MM structure. The frequency drift that happens in the instant 0.15s does not influence on the

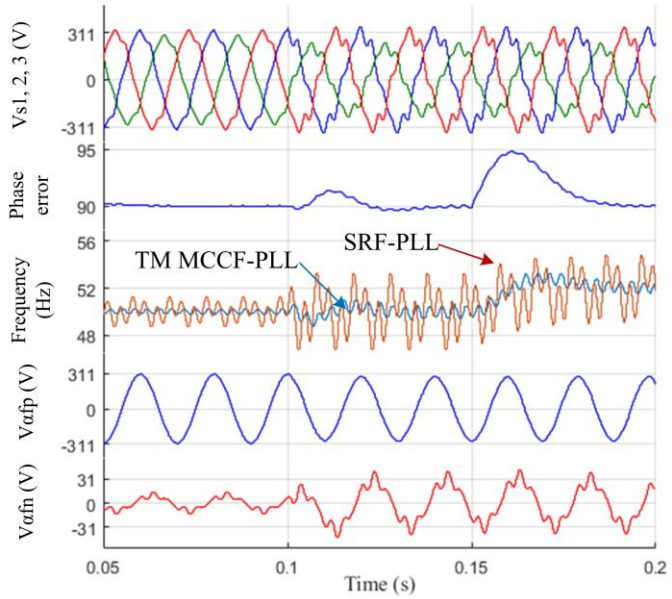

(a)

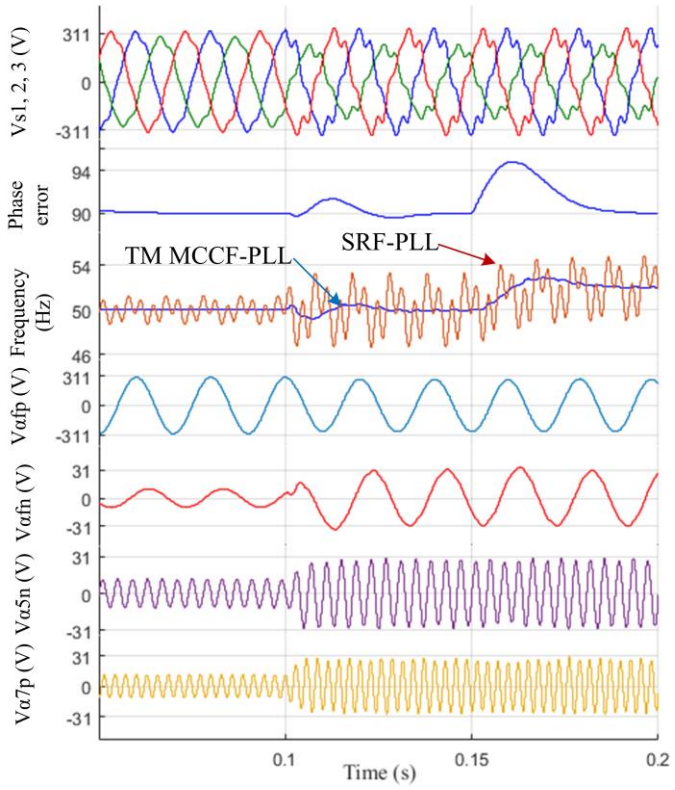

(b)

Fig. 4. Behavior of the MCCF-PLL under unbalanced distorted voltage and frequency excursion. (a) using TM structure. (b) using MM structure.

MCCF-PLL behavior. However, if the grid voltage subjects to a large frequency excursion, then the adaption of the CCFs with the new estimated frequency that is depicted in Fig. 1 is mandatory. Since the objective of the MCCF structure is to extract $v_{\alpha 1}^{p}$ and feed it to the SRF-PLL, then the TM structure is suitable under small perturbation as it provide less computation burden. But in case where the information about the positive and negative sequences is important or the grid perturbation is significant, the

Table I. parameters of the simulation and practical system

Source	Grid Voltages RMS values:	
	Fundamental :	V_s = 230 V
	-5^{th} harmonic:	$V_{-5} = 40$ V
	7^{th} harmonic:	$V_7 = 30$ V
	-11^{th} harmonic:	$V_{-11} = 20$ V
	13^{th} harmonic:	$V_{13} = 10$V
	Main impedance:	$L_s = 0.005\, mH$
		$R_s = 0.5\, \Omega$
	Unbalance	$V_{s1} = 180$ V
		$V_{s1,3} = 230$ V
Shunt active power filter	dc link capacitor:	C = 2200 μF
	dc link voltage references	$V_{dc} = 650$ V
	output filters:	$L_f = 15\, mH$
		$R_f = 2\, \Omega$
Load	Non-linear load:	$R_L = 153\ \Omega$
		$L_L = 10$ mH

MM structure is necessary. The interesting fact of the grid harmonic components is that when their frequencies increase, their amplitudes decrease. Therefore, the number of submodules that corresponds to the most dominant harmonic components is sufficient to provide accurate phase/frequency estimation.

B. *Application of the MCCF-PLL to the SAPF*

Fig. 5 depicts the prototype of the SAPF used in both simulation and practical. It is consisted of three phase source, non-linear load which draws a distorted source current $i_{s1,2,3}$, and a SAPF to compensate for the harmonic distortion. The parameters of the system are presented in Table I. Fig. 6(a) shows the performance of the SRF-PLL under distorted grid voltage $V_{s1,2,3}$. It is obvious when $V_{s1,2,3}$ is ideal, the SRF-PLL offers an accurate phase angle estimation ($\hat{\theta}$) to perform Park transform of $i_{l1,2,3}$. As a results, i_{dac} is accurately separated from i_{ddc} using the MAF, and thus, the RCC generated by the SAPF improves the total harmonic distortion (THD) of $i_{s1,2,3}$ from 29% to 3.6% which respects the IEC 61000-3-6 and IEEE 519-1992 standards. However, when $V_{s1,2,3}$ gets distorted by the -5th, 7th, -11th, and 13th harmonic components in the instant 0.1s with a THD of 12.3%, the SRF-PLL performance degrades. Consequently, the estimation of $\hat{\theta}$ is affected by the harmonic distortion. Even though, the MAF is performing well in separating between i_{dac} and i_{ddc}, the low precision of estimating $\hat{\theta}$ affects the wave form of i_{dac}. As a result, the RCC generated by the SAPF are affected by the harmonic components of $V_{s1,2,3}$, which leads to increase

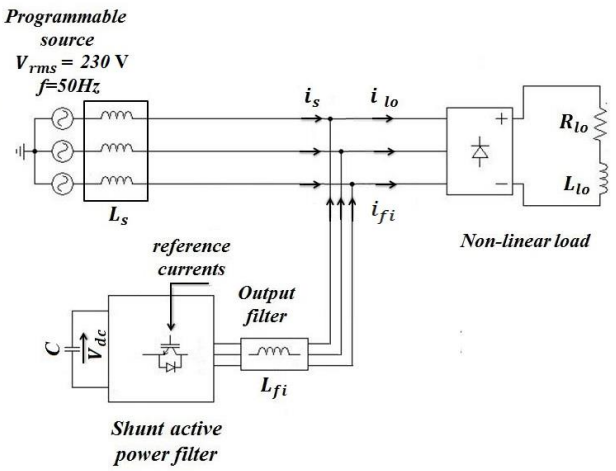

Fig. 5. Simulation and experimental prototype of the SAPF

the THD of $i_{s1,2,3}$ from 3.6% to 12.5%. Fig. 6(b) presents the performance of the MCCF-PLL under distorted grid voltage. Since the voltage distortion is not very high, using only 4 submodules of the MCCF structure set to the fundamental frequency positive and negative sequences and the most dominant harmonic components (-5th and +7th) is sufficient to provide an accurate estimation of $\hat{\theta}$. It is clear that in the instance 0.1s when $V_{s1,2,3}$ gets affected by the harmonic components (-5th, +7th, -11th, +13th), the MCCF-PLL keeps estimating an accurate estimation of $\hat{\theta}$. Supplying $\hat{\theta}$ to the SRF approach results in extracting a correct RCC that keeps the THD of $i_{s1,2,3}$ acceptable (3.6%) and respects the aforementioned standards.

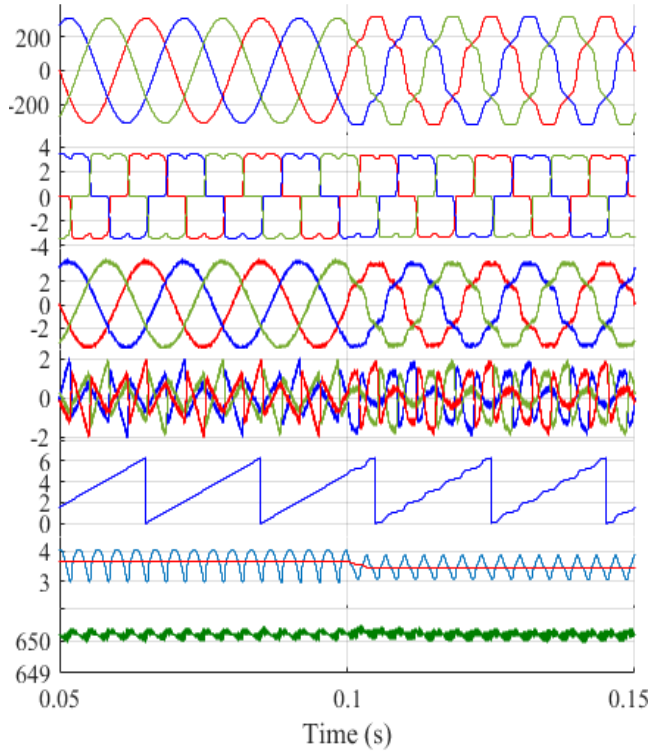

(a)

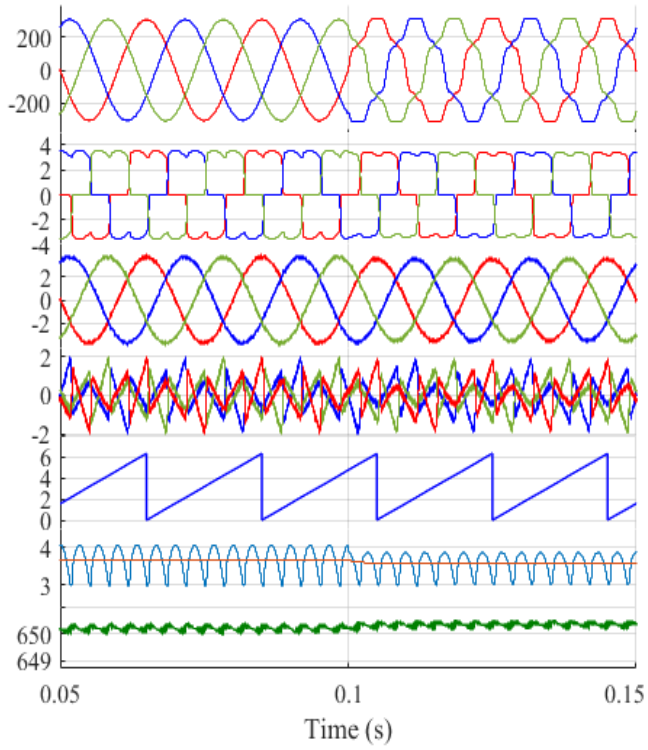

(b)

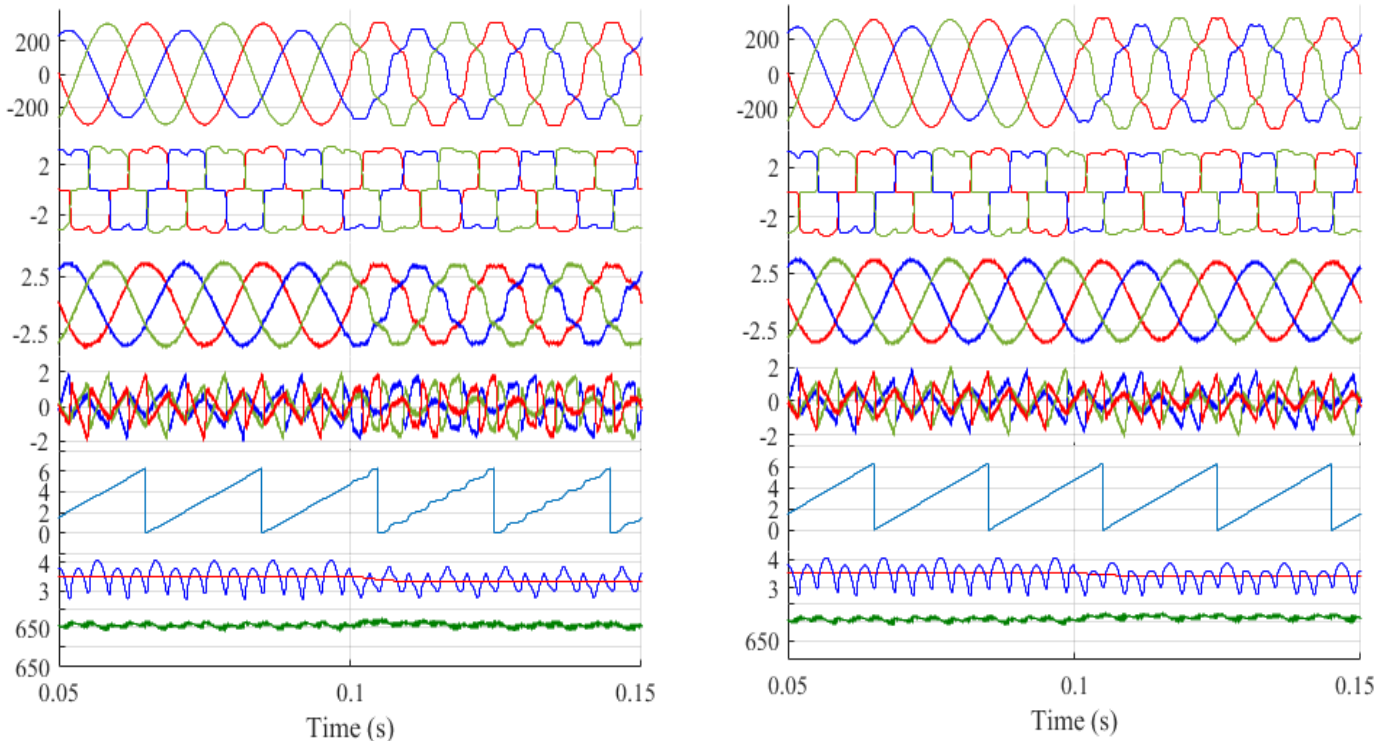

Fig. 6. Simulation results for the case of distorted voltage ((a) and (b)) and distorted and unbalanced voltage ((c) and (d)) using SRF-PLL ((a) and (c)) and MCCF-PLL ((b) and (d)). The subplots are respectively displaying: the perturbed grid voltage, the distorted load current, the compensated source current, the SAPF compensating currents, the voltage phase angle extracted by the PLL, the direct fluctuated and filtered current, and finally the dc link voltage.

Fig. 6(c) and (d) depict, respectively, the performance of the SRF-PLL and MCCF-PLL under unbalanced and distorted voltage with a THD of 12.3% and an unbalance of 9%. It is obvious that a small unbalance does not cause a serious degradation of estimating $\hat{\theta}$ using the SRF-PLL. However, when the perturbation happens in the instance 0.1s, the SRF-PLL shows a weakness in estimating an accurate value of $\hat{\theta}$. Subsequently, the synchronization of the RCC is affected by the perturbation of $V_{s1,2,3}$, and thus the THD of $i_{s1,2,3}$ is augmented from 4.1% to 12.6%. However, estimating $\hat{\theta}$ by the MCCF-PLL is accurate before and after the distortion appears in the unbalanced grid voltage. Therefore, the synchronization of the RCC is achieved with the correct phase estimation of the fundamental positive sequence, which yields to obtain an acceptable THD (3.7%) of $i_{s1,2,3}$ that respects the abovementioned standards.

IV. PRACTICAL RESULTS

The experimental setup consists of a three-phase programmable source (Chroma, model 61845) and a three-phase Danfoss inverter 2.2 kVA with an output L filter. The switching frequency is 10 kHz, the control algorithm is established under MATLAB/Simulink and implemented in a digital signal processor (dSPACE 1006 platform) with a sampling frequency of 10 kHz. The parameters of the experimental setup are presented in Table I.

Fig. 7 presents the experimental behavior of the SAPF under distorted grid voltage and unbalanced distorted grid voltage, using the SRF-PLL (Fig. 7(a) and (c)), and the MCCF-PLL (Fig. 7(b) and (d)). The voltage harmonic distortion is consisted of -5th, 7th, -11th, and 13th harmonic components. The amount of the superposed harmonics and the unbalance are depicted in Table I.

Under ideal grid conditions, the SRF-PLL (Fig. 7(a) and (c)) offers a satisfactory estimation of $\hat{\theta}$ which makes $\cos(\hat{\theta})$ sinusoidal. Consequently, the synchronization of the SRF approach based on Park transform is achieved under ideal conditions, which leads to improve the performance of the SAPF that reduces the THD of $i_{s1,2,3}$ from 29% to around 4.5%. However, when the perturbation occurs, the SRF-PLL cannot offer an accurate estimation of $\hat{\theta}$. This weakness is observable on $\cos(\hat{\theta})$ that is affected by the perturbation of the grid voltage. Thus, the wave shape of $i_{s1,2,3}$ degrades and the THD increases from 4.7% to around 13.8% in case of distorted voltage (Fig. 7(a)), and 14.3% in case of unbalanced and distorted voltage (Fig. 7(c)).

Fig. 7(b) and (d) depict respectively the behavior of the MCCF-PLL under distorted and unbalanced distorted grid voltage. The modules of the MCCF structure are set for the following frequencies: +50 Hz, -50 Hz, -250 Hz, +350 Hz. It is evident that

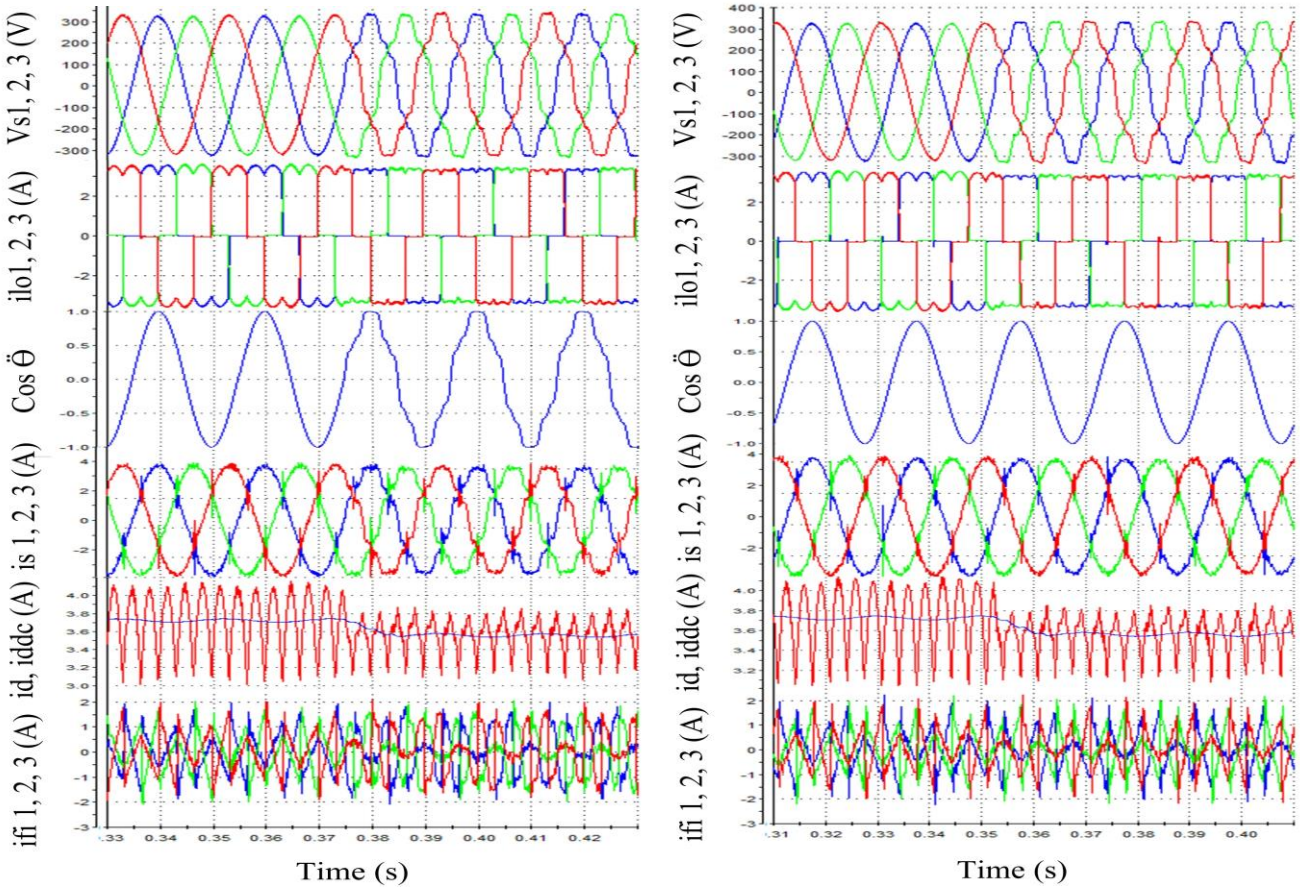

(a) (b)

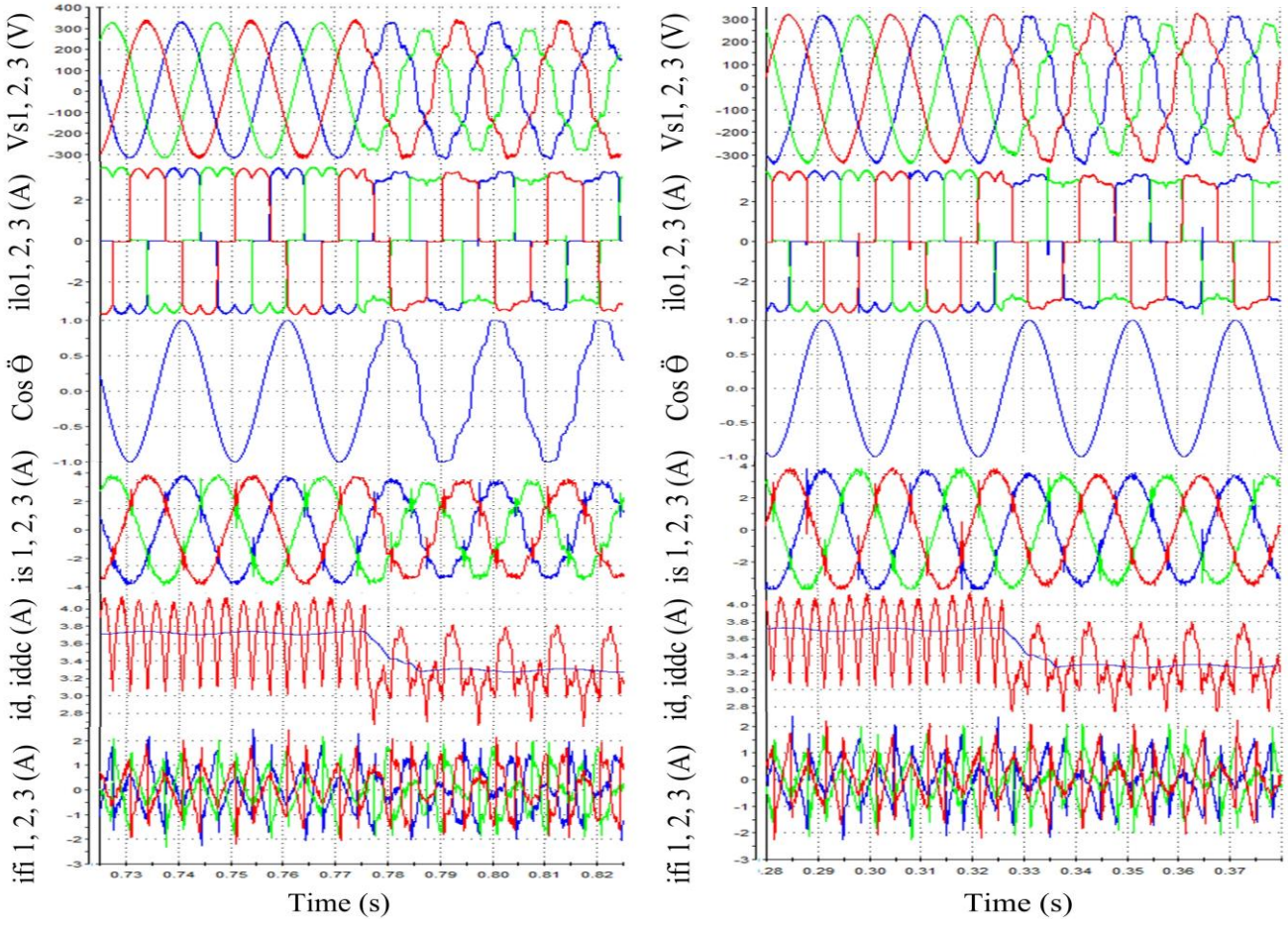

(c) (d)

Fig. 7. Experimental results for the case of distorted voltage ((a) and (b)) and distorted and unbalanced voltage ((c) and (d)) using SRF-PLL ((a) and (c)) and MCCF-PLL ((b) and (d)).

the MCCF-PLL offers an accurate estimation of $\hat{\theta}$ under ideal grid voltage and distorted grid voltage (Fig. 7 (b)),and unbalanced distorted grid voltage (Fig. 7 (d)). The accuracy of the MCCF-PLL emerges on $\cos(\hat{\theta})$ that is maintained sinusoidal even under grid voltage perturbation. The estimated $\hat{\theta}$ of the fundamental positive sequence is fed to the SRF approach to perform the Transform of Park and thus extract the RCC. It is clear that the performance of the SAPF based on MCCF- PLL is improved and keeps the THD of $i_{s1,2,3}$ around 4.7% before and after the perturbation occurs which respects the aforementioned standards.

V. CONCLUSION

According to the conducted studies, the following conclusions are observed from the implimentation of the MCCF-PLL to perform the sychronization of the SAPF with with a distorted and unbalanced grid voltage.

1) The CCFs have valuable advantages of providing information about the polarities of the fundamental and each individual selected harmonic component.

2) Under slightly distorted grid conditions, using only two submodules, or adding extra ones for the most dominat harmonic components are sufficient for providing accurate information about the grid voltage phase\frequency. This property makes the MCCF sutructure a cost effective technique.
3) Although the MCCF sutructre is a pre-filtering technique (implemented in the stationary αβ frame), the feed back of the estimated frequency makes the CCFs adaptive with the frequency variations.
4) In most cases, the grid voltage fundamental positive sequence is fixed, and the negative sequence and other harmonic components are variable due to the affection caused by the variation of loads. Therefore, this variation does not affect the transient response of estimating the phase angle of the fundamental positive sequence as shown in the simulation and experimental results. As a consequence, the dynamic response of the SAPF is optmized.

REFERENCES

[1] Smith, Robert L., and Ray P. Stratford. "Power system harmonics effects from adjustable-speed drives" *IEEE Trans. Ind. Appl*., vol. IA-20, no. 4, pp. 973-977, July 1984.

[2] L. Gyugyi and E. C. Strycula, "Active ac power filters," in Proc. IEEE/IAS Ann. Meet., 1976, pp. 529–529.

[3] B. Singh, K. Al-Haddad and A. Chandra, "A review of active filters for power quality improvement," *IEEE Trans. Ind. Electron*., vol. 46, no. 5, pp. 960-971, Oct. 1999.

[4] Abdusalam, Mohamed, et al. "New digital reference current generation for shunt active power filter under distorted voltage conditions." Electric Power Systems Research 79.5 (2009): 759-765.

[5] Saad, S., and L. Zellouma. "Fuzzy logic controller for three-level shunt active filter compensating harmonics and reactive power." Electric Power Systems Research 79.10 (2009): 1337-1341.

[6] L. Asiminoael, F. Blaabjerg and S. Hansen, "Detection is key - Harmonic detection methods for active power filter applications," *IEEE Ind. Appl. Mag*., vol. 13, no. 4, pp. 22-33, July-Aug. 2007.

[7] F. Corasaniti, B. Barbieri and P. Arnera, "Compensation with Hybrid Active Power Filter in an Industrial Plant," *IEEE Latin America Transactions*, vol. 11, no. 1, pp. 447-452, Feb. 2013.

[8] P. Dey and S. Mekhilef, "Current harmonics compensation with three-phase four-wire shunt hybrid active power filter based on modified D–Q theory," in IET Power Electronics, vol. 8, no. 11, pp. 2265-2280, 11 2015.

[9] M. Boyra, and J. L. Thomas, "A review on synchronization methods for grid-connected three-phase VSC under unbalanced and distorted conditions," in Proc. 14th Eur. Conf. Power Electron. Appl., Birmingham, U.K., Aug. 2011, pp. 1-10.

[10] P. Rodríguez, R. Teodorescu, I. Candela, A. V. Timbus, M. Liserre and F. Blaabjerg, "New positive-sequence voltage detector for grid synchronization of power converters under faulty grid conditions," 2006 37th IEEE Power Electronics Specialists Conference, Jeju, 2006, pp. 1-7

[11] L. Shi and M. L. Crow, "A novel PLL system based on adaptive resonant filter," 2008 40th North American Power Symposium, Calgary, AB, 2008, pp. 1-8.

[12] F. Gonzalez-Espin, E. Figueres and G. Garcera, "An adaptive synchronous-reference-frame phase-locked loop for power quality improvement in a polluted utility grid," *IEEE Trans. Ind. Electron*.,vol. 59, no. 6, pp. 2718-2731, June 2012.

[13] F. D. Freijedo, J. Doval-Gandoy, O. Lopez, and E. Acha, "A generic openloop algorithm for three-phase grid voltage/current synchronization with particular reference to phase, frequency, and amplitude estimation," *IEEE Trans. Power Electron*., vol. 24, no. 1, pp. 94–107, Jan. 2009.

[14] E. Robles, S. Ceballos, J. Pou, J. L. Martín, J. Zaragoza and P. Ibañez, "Variable-Frequency Grid-Sequence Detector Based on a Quasi-Ideal Low-Pass Filter Stage and a Phase-Locked Loop," *IEEE Trans. Power Electron*., vol. 25, no. 10, pp. 2552-2563, Oct. 2010.

[15] Y. F. Wang and Y. W. Li, "Three-Phase Cascaded Delayed Signal Cancellation PLL for Fast Selective Harmonic Detection," IEEE Trans. Ind. Electron., vol. 60, no. 4, pp. 1452-1463, April 2013.

[16] S. Golestan, J. M. Guerrero and J. C. Vasquez, "Three-Phase PLLs: A Review of Recent Advances," *IEEE Trans. Power Electron*., vol. 32, no. 3, pp. 1894-1907, March 2017.

[17] K. W. Martin, "Complex signal processing is not complex," *IEEE Trans. Circuits Syst. I, Reg. Papers*., vol. 51, no. 9, pp. 1823–1836, Sep. 2004.

[18] X. Guo, W. Wu, and Z. Chen, "Multiple-complex coefficient-filter-based phase-locked loop and synchronization technique for three-phase grid-interfaced converters in distributed utility networks," *IEEE Trans. Ind. Electron*., vol. 58, no. 4, pp. 1194–1204, Apr. 2011.

[19] S. Golestan, M. Monfared and F. D. Freijedo, "Design-Oriented Study of Advanced Synchronous Reference Frame Phase-Locked Loops," *IEEE Trans. Power Electron*., vol. 28, no. 2, pp. 765-778, Feb. 2013.

[20] P. Xiao, K. A. Corzine, and G. K. Venayagamoorthy, "Multiple reference frame-based control of three-phase PWM boost rectifiers under nbalanced and distorted input conditions," *IEEE Trans. Power Electron*., vol. 23, no. 4, pp. 2006–2017, Jul. 2008.

[21] S. Golestan, M. Monfared, F. D. Freijedo and J. M. Guerrero, "Performance Improvement of a Prefiltered Synchronous-Reference-Frame PLL by Using a PID-Type Loop Filter," *IEEE Trans. Ind. Electron*.,vol. 61, no. 7, pp. 3469-3479, July 2014.

[22] S. Preitl and R.-E. Precup, "An extension of tuning relations after symmetrical optimum method for PI and PID controller," Automatica, vol. 35,no. 10, pp. 1731–1736, Oct. 1999

[23] K. Shu and E. Sanchez-Sinencio, CMOS PLL Synthesizers-Analysis and Design. New York: Springer, 2005.